# Investigation of Elastic and Thermodynamic Properties of $XA_2B_4$ (X = Mg, Zn, Cd; A = Sc, Y; B = S, Se) Spinel Compounds

Z. Noor<sup>a</sup>, G. Murtaza<sup>a,\*</sup>, M.A. Jehangir<sup>a</sup> and A.R. Chaudhry<sup>b</sup>

Received: 02.04.2025 & Accepted: 05.08.2025

Doi: 10.12693/APhysPolA.148.77 \*e-mail: murtaza@icp.edu.pk

Spinels have an accurate structure and composition, which allows them to exhibit excellent properties and be used in advanced applications. In this study, using density functional theory calculations, we have examined the less-explored elastic properties of spinal compounds ( $AB_2X_4$ ). All studied compounds are in the cubic phase with a direct bandgap. The different elastic properties of spinal compounds are calculated using the elastic constant  $(C_{ij})$ , i.e., bulk modulus, shear modulus, anisotropy, Poisson's ratio, Cauchy's pressure, Young's modulus, and linear compressibility, etc. The results obtained using the quasiharmonic Debye model show increase in bulk modulus B, Gibbs free energy G and a decreasing trend for the entropy S, showing the thermodynamic stability of the compounds in the range of 200 to 800 K and 0 to 20 GPa.

topics: elastic tensor, elastic moduli, spinel, quasiharmonic Debye model

#### 1. Introduction

The optoelectronic industry primarily relies on semiconductors. The design of a potent optoelectronic device can be effectively launched with the appropriate selection of the required energy band gap of the electromagnetic spectrum in a specific energy range. The finest energy band gap is the one at which the interband transition takes place directly from the valence band to the conduction band. It is therefore easy to theoretically predict and design new materials that have the required attributes to satisfy the continuously growing needs of the technological market.

The common formula of spinel compounds is  $AB_2X_4$ , where A and B represent metal ions such as iron (Fe), zinc (Zn), magnesium (Mg), aluminum (Al), manganese (Mn), chromium (Cr), and titanium (Ti). These metals ions can be divalent, trivalent, or tetravalent cations. In turn, X can be an oxygen (O) or chalcogen ion (sulphur or selenium) with a valency of +2. Star spinels were named "precious stones" due to their rare occurrence. Spinels containing  $Cr^{3+}$  are called red spinels, and those containing  $Zn^{2+}$  and  $Zn^{2+}$  have been termed blue spinels [1].

Spinels represent a group of a very huge family—almost all metals and transition elements form spinels. Due to the unique features, i.e., electronic configurations, manifold compositions, and valence states, spinels have shown intrinsic magnetic properties [2, 3], optical properties [4], electrical properties [5–7], and catalytic properties [8, 9]. In the field of energy storage, spinels have wide-ranging application in the form of supercapacitors [10] and metal-ion batteries [11]. The most important use of spinels compounds with magnesium ions [12], sodium ion [13], and zinc ions [14] are electrodes. For catalytic reactions, spinels are the best option due to their manageable composition, structure, valence, and morphology.

 $AB_2X_4$  type spinel materials have captured the market attention [15, 16], since they exhibit a unique range of physical properties, including a significant phase transition [17], transparent character over a longer energy range, as well as extraordinary (high) photosensitivity [18], nonlinear optical susceptibility and birefringence [19], colossal magneto resistance [20], partial metallicity [21], metal—insulator transition [22], the ability to sense humidity [23], optimum catalytic activity [24], charge storage potential [25], and thermoelectricity [26], etc. These unique features associated with

<sup>&</sup>lt;sup>a</sup> Materials Modelling Lab, Department of Physics, Islamia College Peshawar, P.O. Box 25120, Pakistan

<sup>&</sup>lt;sup>b</sup>Department of Physics, College of Science, University of Bisha, P.O. Box 551, Bisha 61922, Saudi Arabia

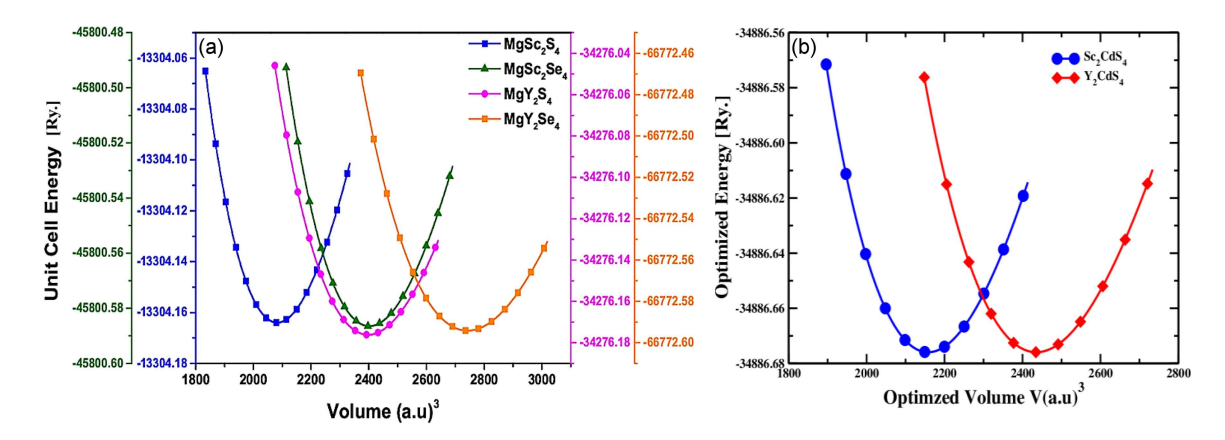


Fig. 1. (a, b) Equation of state (EOS) of the compounds.

spinels attract attention because they are considered extremly valuable in the device industry for multiple applications [27–33].

Thiospinels play an important role in the study of defect engineering, particularly under pressure under certain conditions [34]. It is a requirement of the present time to search for new uses of semiconductors in optoelectronic devices. The physical properties and synthesis of MgSc<sub>2</sub>Se<sub>4</sub> and MgY<sub>2</sub>Se<sub>4</sub> were studied by Guittard et al. [35] by using a 2-step procedure. Theoretically, Canepa et al. [36] investigated the computational and measured data of the mobility of magnesium ions while studying spinel compounds. Hence, they testified and verified the practicality of MgSc<sub>2</sub>Se<sub>4</sub> for batteries based on magnesium ions. Moreover, Wang et al. [37] also synthesized MgSc<sub>2</sub>Se<sub>4</sub> and then subsequently determined its electronic and ionic conductivities. The defects present intrinsically and extrinsically in MgSc<sub>2</sub>S<sub>4</sub> and MgSc<sub>2</sub>Se<sub>4</sub> were studied by Canepa et al. [38]. All spinels of the form  $MgA_2B_4$  (A = Sc, Y; B = S, Se) were found to be of semiconductors nature [39].

In this work, chalcogenide-based spinel compounds are studied using density functional theory (DFT). Our calculations focused on the elastic properties of spinal compounds of the form  $AB_2X_4$ . All of these compounds are in the cubic phase with a direct bandgap. The uniqueness of this work is in bringing forward new characteristics for materials that could have applications in advance technology. This work, in addition to other important aspects, could fill a gap resulting in the lack of sufficient theoretical data on spinel compounds.

### 2. Computational detail

The first principles study of the materials is carried out based on the full potential augmented plane wave plus local-orbital (FP-LAPW+lo) [40] method implemented in the WIEN2K code [41]. In

this method, the crystal's unit cell is divided into two portions. In the first portion, we have nonoverlapping spheres called the muffin tin  $(R_{\rm MT})$ spheres, and in the second portion, we have the interstitial region. The charge density and wave functions are to be treated differently in these two regions. Elastic, structural, and mechanical properties are studied using the generalized gradient approximation (GGA) [42]. Since a large number of spinel materials are studied in the present work, therefore the muffin tin radii  $R_{\rm MT}$  of the elements is chosen in such a way that no charge is leaked from the core in all materials. The size of the basis set  $(R_{\rm MT} K_{\rm max})$  for the calculations is set to 7. The size of the maximum vector  $\boldsymbol{G}$  in the Fourier expansion is set to 12. The cutoff energy for the calculations is -6.0 Ry, and the criteria for charge and energy convergence are set to 0.0001e and 0.0001 Ry, respectively. A dense mesh of K points is necessary to achieve Brillouin zone integrations. A mesh of 1000K points is selected to perform the Brillouin zone integrations.

# 3. Results and discussion

### 3.1. Structural and mechanical properties

As elastic constants are very closely related to the ground-state properties of materials, in order to obtain accurate and reliable results, the lattice constants are optimized for the chosen cubic spinel compounds based on transition metal chalcogenides:  $MgA_2B_4$ ,  $ACd_2S_4$ , and  $ZnA_2B_4$  (where  $A=Sc,\ Y$  and  $B=S,\ Se$ ). The unit cell energy of the crystal varied with the unit cell volume over a specific range. The Birch–Murnaghan equation of state is used for the energy corresponding to the unit cell volume; the results of the E-V dependence are shown in Fig. 1.

The decrease in energy of a unit cell occurs with increase in unit cell volume and approaches its lowest value at the ground state. Thereafter,

TABLE I

DFT optimized lattice constant  $a_0$  [Å], ground state energy  $E_0$  along with ground state volume,  $V_0$  for spinel compounds  $MgA_2B_4$  (A = Sc or Y; B = S or Se),  $ACd_2S_4$ , and  $ZnA_2B_4$  in comparison with the experiment values.

Compounds	$a_0$ [Å]	$V_0 [(a.u)^3]$	$E_0$ [eV]	
	10.72	2082.81	-13304.16	
$MgSc_2S_4$	$10.63^{a}$			
	$10.62^{b}$			
	11.25	2402.11	-45800.58	
${ m MgSc_2Se_4}$	$11.14^{c}$			
	$11.12^{d,e}$			
$\overline{\mathrm{MgY_2S_4}}$	11.18	2397.69	-34276.17	
$\overline{\mathrm{MgY_{2}Se_{4}}}$	11.69	2742.21	-66772.59	
$CdSc_2S_4$	10.85	2157.64	-34887	
$CdY_2Se_4$	11.31	2441.99	-55859	
$ZnSc_2S_4$	10.62	2020.96	-19687	
21130234	$10.40^{f}$			
ZnSc <sub>2</sub> Se <sub>4</sub>	11.10	2309.26	-52183	
ZII3C25e4	$10.88^{g}$			
$ZnY_2S_4$	11.29	2431.85	-40659	
ZII I 254	$10.87^{h}$			
7nV Co	11.58	2623.75	-73155	
$\mathrm{ZnY}_{2}\mathrm{Se}_{4}$	$11.34^{h}$			

 $<sup>{}^</sup>a{\rm Ref.~[43]}, \ {}^b{\rm Ref.~[44]}, \ {}^c{\rm Ref.~[45]}, \ {}^d{\rm Ref.~[46]}, \ {}^e{\rm Ref.~[47]},$   ${}^f{\rm Ref.~[48]}, \ {}^g{\rm Ref.~[49]}, \ {}^h{\rm Ref.~[50]}$ 

the energy of a unit cell grows with increasing unit cell volume, forming a parabolic curve. The calculated results of the lattice constants a [Å], ground state energy  $E_0$  [eV], and other structural parameters found during these studies are presented in Table I. These lattice parameters values were then used for performing the computation of the elastic constants. The results of  $C_{11}$ ,  $C_{12}$ , and  $C_{44}$ — representing the elastic constants for all compounds  $MgA_2B_4$  (A = Sc, Y; B = S, Se),  $ACd_2S_4$ , and  $ZnA_2B_4$  — are given in Table II together with previous theoretical and experimental data. To the best of our knowledge, the experimental data are lacking for most of the substances, except for ScCd<sub>2</sub>S<sub>4</sub>, YCd<sub>2</sub>S<sub>4</sub>, ZnY<sub>2</sub>S<sub>4</sub>, and ZnY<sub>2</sub>Se<sub>4</sub>. Our calculations of the elastic constants and other elastic parameters show good agreement with other experimental and theoretical data given in Table II. This is a clear indication that compounds satisfy the requirement for stability of cubic structures, given by

$$C_{11} > 0,$$
  $C_{44} > 0,$   $(C_{11} + 2C_{12}) > 0,$   $C_{11} - C_{12} > 0.$  (1)

Hence, all spinel compounds under study are stable with respect to elastic deformation.

Using three elastic constants, i.e.,  $C_{11}$ ,  $C_{12}$ , and  $C_{44}$ , the elastic properties of cubic spinels  $AB_2X_4$  (A = Mg, Zn, Cd; B = Sc or Y; and X = S or Se) have been calculated. For cubic compounds, these three elastic constants are suitable for the extraction of important elastic parameters such as stiffness, ductility, degree of anisotropy A, Lame constant  $\lambda$ , Grüneisen parameter  $\gamma$ , Voigt-Reuss-Hill modulus  $G_V$  and  $G_R$ , Cauchy's pressure  $C_P$ , bulk modulus B, shear modulus G, Young's modulus Y, and Poisson's ratio v. A set of constraints on the elastic constants  $(C_{ij})$  [51] constitutes the Born stability criteria given by (1). These conditions were satisfied, demonstrating the mechanical stability of the material. Furthermore, to compute the elastic moduli, i.e, B, G, and Y, and Poisson's ratio v, the following formulas are used

$$B = \frac{C_{11} + 2C_{12}}{3},\tag{2}$$

$$G = \frac{G_V + G_R}{2},\tag{3}$$

$$Y = \frac{9BG_V}{3B + G_V},\tag{4}$$

$$v = \frac{3B - 2G}{2(3B + 2G)}. (5)$$

Reuss modulus  $(G_R)$ , Voigt modulus  $(G_V)$ , fracture energy (R), and fracture toughness (K) could also be easily calculated with the use of

$$G_R = \frac{5C_{44}(C_{11} - C_{12})}{4C_{44} + 3(C_{11} - C_{12})},\tag{6}$$

$$G_V = \frac{1}{5} \left( C_{11} - C_{12} + 4C_{44} \right), \tag{7}$$

$$K = 1/B. (8)$$

The calculated values of the bulk moduli B presented in Table II decrease down the column and are in good agreement with previous works [50, 52, 53]. It can be seen that the compounds  $MgY_2Se_4$ ,  $MgSc_2Se_4$ ,  $ZnY_2S_4$ , and  $ZnY_2Se_4$  are more compressible than  $ZnSc_2Se_4$  and  $CdY_2S_4$ , and that  $ZnSc_2Se_4$  and  $CdY_2S_4$  are more compressible than  $MgSc_2S_4$ ,  $MgY_2S_4$ ,  $CdSc_2S_4$ , and  $ZnSc_2S_4$ . The compound  $MgSc_2S_4$  exhibits a superior bulk modulus (76.96 GPa) relative to the other compounds, which indicates a greater resistance to volumetric alterations.

The shear modulus G [GPa] has been used to quantify the ability of a substance to endure geometric deformations when subjected to shear stress. Calculated values of shear modulus G for all groups of spinel compounds are given in Table II. The compound  $\rm ZnSc_2S_4$  has the greatest value (51.33 GPa), while  $\rm ZnY_2Se_4$  has the lowest value (34.30 GPa), as shown in Fig. 2. The property known as Young's modulus (Y) indicates the rigidity of a polycrystalline material. A higher Y value indicates that the

TABLE II Elastic constants  $C_{ij}$  [GPa], bulk modulus B [GPa], Reuss modulus  $G_R$  [GPa], Voigt modulus  $G_R$  [GPa], shear modulus [GPa], and tetragonal shear modulus G'.

Compounds	$C_{11}$	$C_{12}$	$C_{44}$	В	$G_V$	$G_R$	G	G'
${ m MgSc_2S_4}$	151.74	39.58	40.73	76.96	46.87	45.37	46.30	56.08
${ m MgSc2Se_4}$	138.94	27.68	29.71	64.77	40.08	36.51	38.29	55.63
${ m MgY_2S_4}$	175.91	25.66	28.82	75.74	47.34	38.25	42.79	75.12
	$85.55^{a}$	$48.02^{a}$	$30.08^{a}$	$60.53^a$			$24.89^{a}$	
	149.66	19.96	24.92	63.19	40.89	33.07	36.98	64.8
$MgY_2Se_4$	$78.08^{b}$	$55.47^{b}$	$24.57^{b}$	$63.00^{b}$			$19.26^{b}$	
	$69.62^a$	$42.03^{a}$	$24.28^{a}$	$51.23^{a}$			$19.35^{a}$	
$\mathrm{Sc_{2}CdS_{4}}$	147.16	40.01	40.71	75.73	45.86	45.04	45.44	53.57
$Y_2CdSe_4$	138.26	31.87	32.68	67.34	40.88	38.64	39.76	53.19
$ZnSc_2S_4$	165.51	31.01	42.80	75.84	52.58	50.09	51.33	67.25
$\mathrm{ZnSc_{2}Se_{4}}$	156.35	21.31	35.72	66.32	48.44	44.01	46.22	67.52
$ m ZnY_2S_4$	149.61	19.88	22.77	63.12	39.61	30.76	35.18	64.86
	$146.6^{c}$	$34.2^c$	$36.4^{c}$		$71.70^{c}$		$43.40^{c}$	
$ m ZnY_2Se_4$	157.50	19.00	20.55	65.17	40.03	28.59	34.30	69.25
	$108.7^{c}$	$20.5^{c}$	$28.00^{c}$	$59.00^{c}$			$31.40^{c}$	

<sup>&</sup>lt;sup>a</sup>Ref. [51], <sup>b</sup>Ref. [52], <sup>c</sup>Ref. [50]

TABLE III Lame coefficients  $\lambda$  and  $\mu$ , Young's modulus Y [GPa], Kleinman parameter  $\zeta$ , Poisson's ratio v, melting temperature  $T_m$  [K], Pugh's ratio B/G, Zener anisotropy parameter A, Cauchy pressure  $C_P$ .

Compounds	Y	v	B/G	$C_P$	A	$T_m$	ζ	λ	$\mu$
$MgSc_2S_4$	115.70	0.25	1.66	-1.14	0.72	1449.78	0.46	46.1	46.3
$MgSc_2Se_4$	95.97	0.25	1.69	-2.02	0.53	1374.14	0.38	39.23	38.3
${ m MgY}_2{ m S}_4$	108.03	0.26	1.77	-3.15	0.38	1592.61	0.32	47.21	42.79
	$65.67^{a}$		$2.43^{a}$						
	92.83	0.26	1.71	-4.96	0.38	1437.5	0.3	38.54	36.98
${ m MgY}_2{ m Se}_4$	$52.44^{b}$	$0.36^{b}$	$3.27^{b}$						
	$51.55^{a}$		$2.65^{a}$						
$\mathrm{CdSc_{2}S_{4}}$	113.61	0.25	1.67	-0.70	0.75	1422.73	0.47	45.43	45.45
$\mathrm{CdY_{2}Se_{4}}$	99.66	0.25	1.69	-0.80	0.61	1370.13	0.42	40.83	39.76
$ZnSc_2S_4$	125.65	0.22	1.48	-11.79	0.63	1531.15	0.37	41.62	51.33
$ZnSc_2Se_4$	112.53	0.22	1.43	-14.41	0.52	1477.02	0.3	35.5	46.23
$ZnY_2S_4$	89.01	0.26	1.79	-2.89	0.35	1437.21	0.3	39.67	35.18
ZIII 254	$108.3^{c}$	$0.25^{c}$	$1.65^{c}$			$1419.00^{c}$			
ZnY <sub>2</sub> Se <sub>4</sub>	87.56	0.28	1.90	-1.54	0.29	1483.84	0.29	42.3	34.31
ZIII 25e4	$79.9^{c}$	$0.27^{c}$	$1.88^{c}$			$1195.00^{c}$			

 $<sup>{}^{</sup>a}$ Ref. [51],  ${}^{b}$ Ref. [52],  ${}^{c}$ Ref. [50]

material exhibits greater stiffness and hardness, as well as enhanced resistance to mechanical deformation. Table III shows that the compound  $\rm ZnSc_2S_4$  has the highest Y value among all, while the compound  $\rm ZnY_2Se_4$  has the lowest one. This indicates that  $\rm ZnSc_2S_4$  is stiffer, harder, and more resistant to any deformation, as shown in Fig. 3. The important parameter is the shear constant G', which describes the dynamical stability of the compounds and indicates the stability against tetragonal distortion.

The G' values for the compounds are presented in Table II and also are compared with other results [50, 52, 53].

The Cauchy pressure  $C_P$  is an important elastic parameter for the angular characteristic of atomic bonding, as described in [54]. Ionic bonding is associated with a positive value of  $C_P$ , whereas covalent bonding is caused by its negative value. Increases in negative values of  $C_P$  indicate stronger directed bonding, which results in a material with

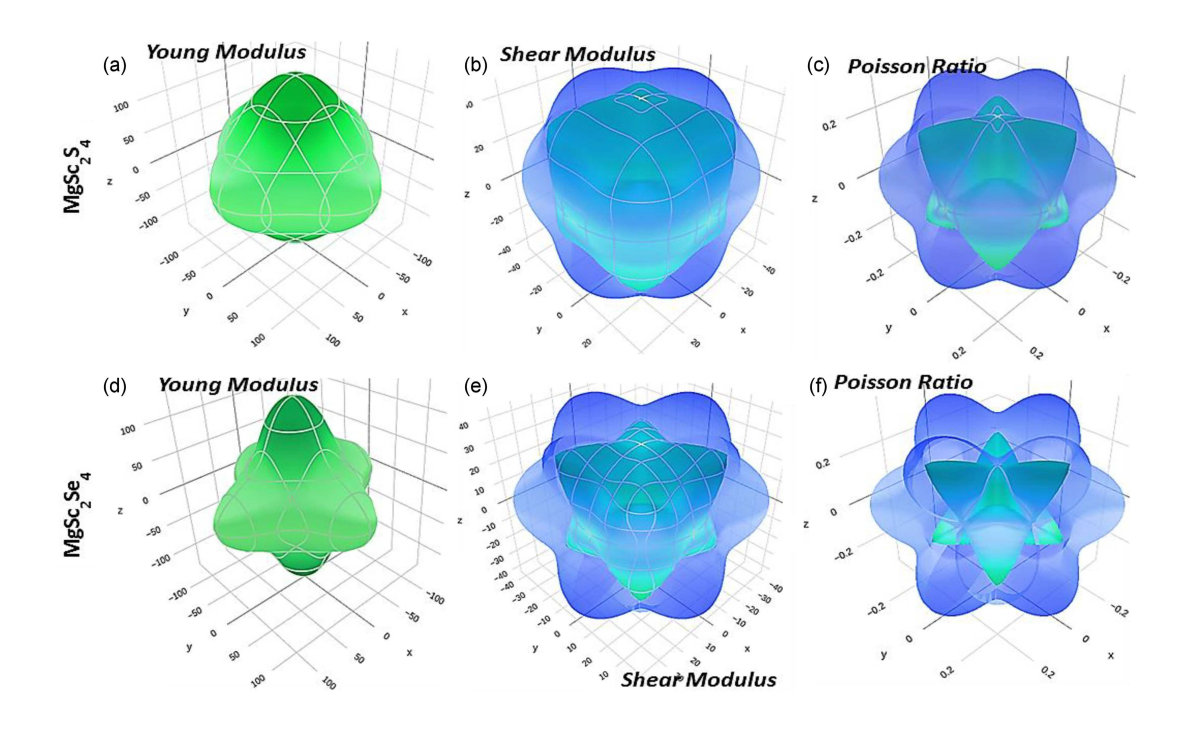


Fig. 2. (a, d) Young modulus, (b, e) shear modulus, and (c, f) Poisson ratio of the spinel MgSc<sub>2</sub>(S/Se)<sub>4</sub>.

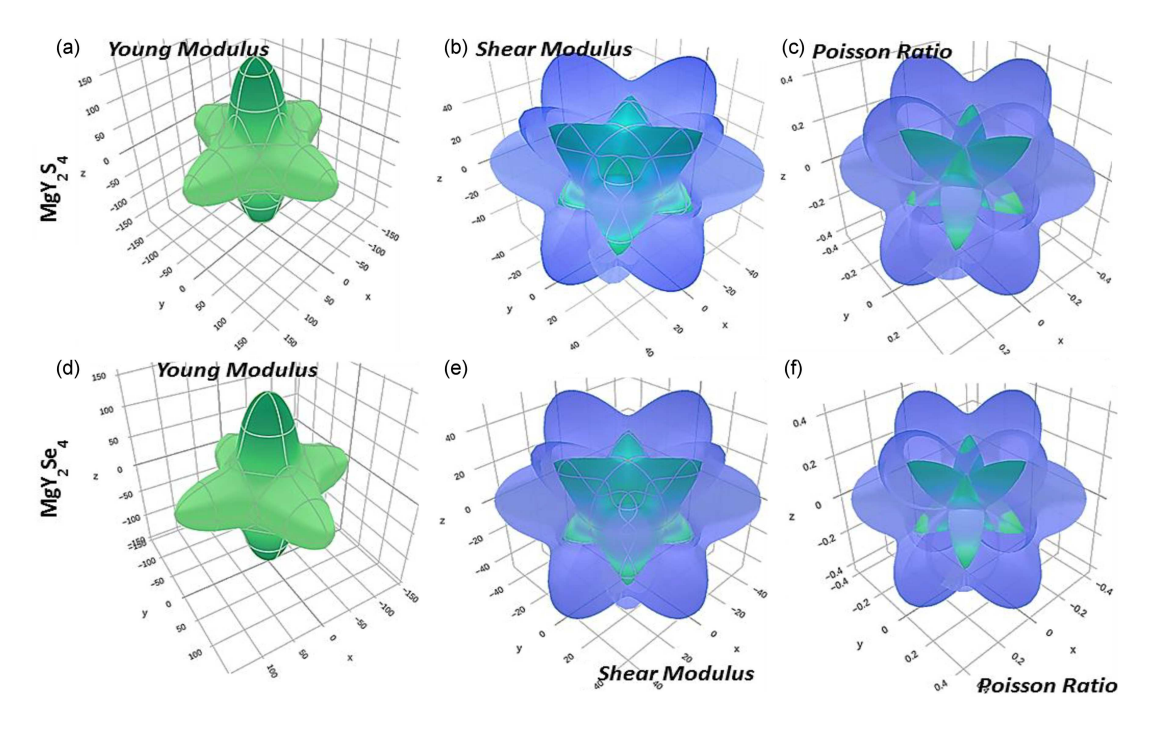


Fig. 3. (a, d) Young modulus, (b, e) shear modulus, and (c, f) Poisson ratio of the spinel MgY<sub>2</sub>(S/Se)<sub>4</sub>.

a reduced mobility characteristic. Table III presents the Cauchy pressure values calculated with the equation  $C_P = C_{12} - C_{44}$ ; they are all negative, showing that spinel compounds have covalent bonding and a brittle nature, as  $C_P < 0$ .

Poisson ratio (v) [55] and Pugh's ratio (B/G) [56] help determine the ductile or brittle nature of a material. If v > 0.26 and B/G > 1.75, the material

represents a ductility nature. For the compound  $\rm ZnY_2Se_4$ , one has  $\upsilon > 0.26$ , and for  $\rm MgY_2S_4$ ,  $\rm ZnY_2S_4$ , and  $\rm ZnY_2Se_4$ , B/G exceed the critical value of 1.75, as shown in the three-dimensional (3D) plots in Figs. 4–6. This is a clear indication of the ductile nature of the  $\rm ZnY_2Se_4$  material, while the rest of the compounds in this series show a brittle nature, as illustrated in Table III. 3D plots of

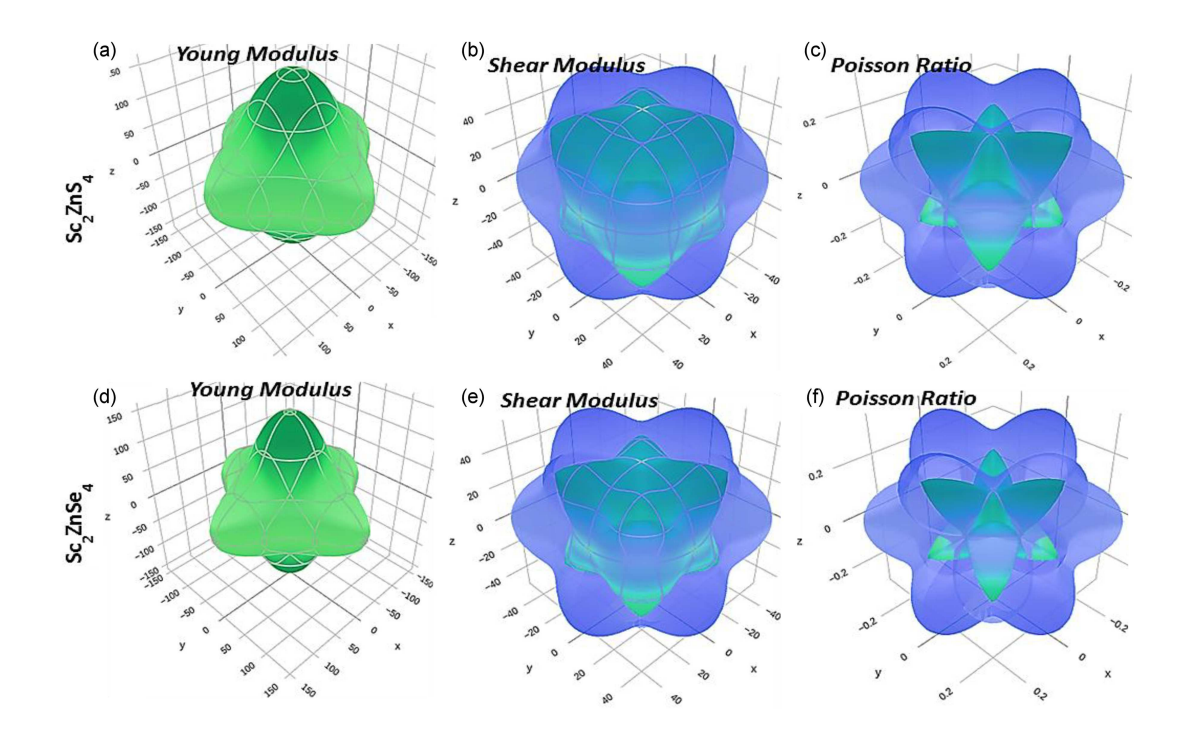


Fig. 4. (a, d) Young modulus, (b, e) shear modulus, and (c, f) Poisson ratio of the spinel ZnSc<sub>2</sub>(S/Se)<sub>4</sub>.

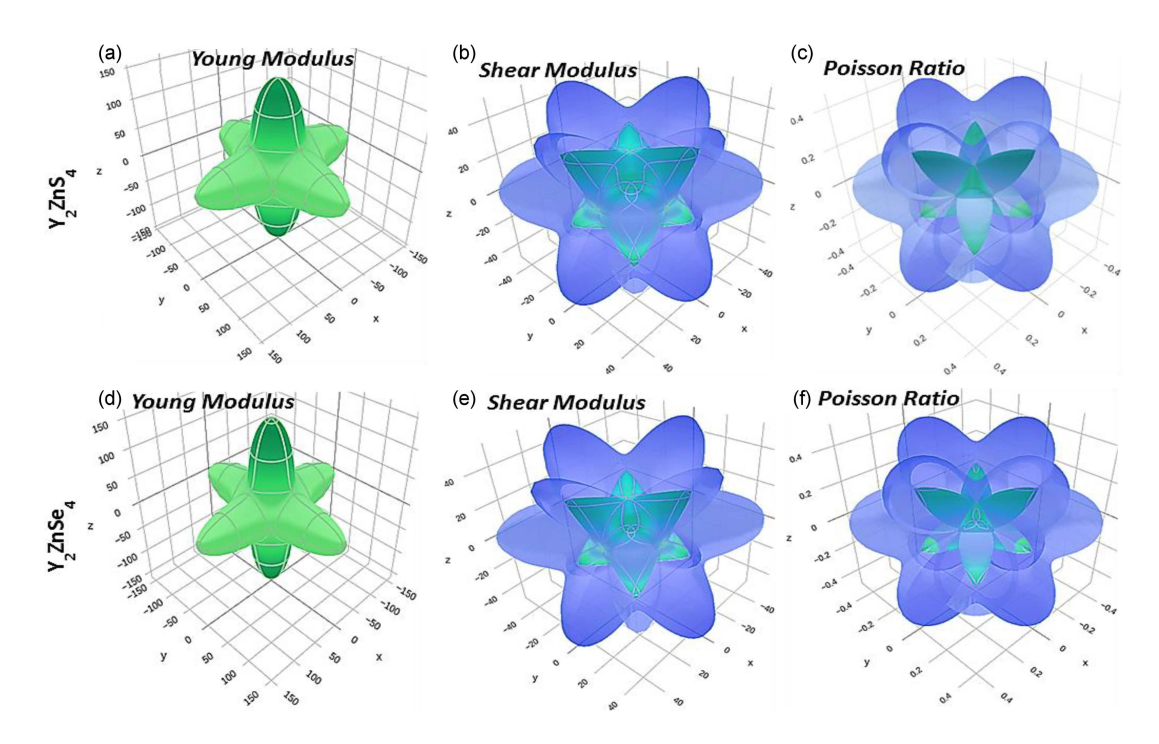


Fig. 5. (a, d) Young modulus, (b, e) shear modulus, and (c, f) Poisson ratio of the spinel ZnY2(S/Se)4.

elastic properties are becoming a powerful means of visualizing how a material's mechanical behavior, such as stiffness or compliance, changes with direction. The plots are particularly important in analysing anisotropic materials, including crystals and composites, whose properties differ with orientation. In such plots, the x, y, and z axes correspond to Cartesian coordinates, and the radial distance

from the origin to the surface in any direction represents the magnitude of the elastic property in that specific direction.

The degree of elastic anisotropy of a material is measured by its Zener factor (A) given as

$$A = \frac{2C_{44}}{(C_{11} - C_{12})}. (9)$$

TABLE IV Debye temperature  $\Theta_{\rm D}$  [K], Grüneisen parameters  $\gamma$ , density  $\rho$  [g/cm<sup>3</sup>], transverse velocity  $V_t$ , longitudinal velocity  $V_t$ , mean acoustic sound velocity  $V_m$ , and compressibility K [GPa<sup>-1</sup>].

Compounds	$\Theta_{\mathrm{D}}$ [K]	γ	$ ho \ [{ m g/cm^3}]$	$V_t$ [m/s]	$V_l$ [m/s]	$V_m$ [m/s]	$K [\mathrm{GPa}^{-1}]$
$\frac{1}{\mathrm{MgSc_2S_4}}$	850.18	1.04	2.63	8802.56	7262.06	8149.22	0.012
$MgSc_2Se_4$	488.6	1.04	4.04	4739.58	5354.42	4912.91	0.015
$MgY_2S_4$	669.31	1.02	3.14	6814.16	6503.26	6703.96	0.013
${ m MgY_2Se_4}$	428.29	1.03	4.29	4310.05	5120.95	4522.82	0.015
$CdSc_2S_4$	627.41	1.04	3.45	6586.75	6286.06	6480.17	0.013
$CdY_2S_4$	513.88	1.04	3.84	5177.23	5598.34	5303.43	0.014
$\mathrm{ZnSc_{2}S_{4}}$	789.28	1.08	3.21	7996.07	6704.4	7458.54	0.013
$ZnSc_2Se_4$	513.44	1.09	4.61	5013.82	5268.42	5093.19	0.015
$ m ZnY_2S_4$	503.17	1.02	3.68	4780.24	5468.13	4970.77	0.015
	$400^{a}$			$6210.00^a$	$3600.00^a$	$4000.00^a$	
$ m ZnY_2Se_4$	370.56	1.00	4.81	3566.41	4801.99	3836.66	0.015
2111 25 64	$284.00^{a}$			$4750.00^a$	$2650.00^a$	$2950.00^a$	

 $<sup>{}^{</sup>a}$ Ref. [50]

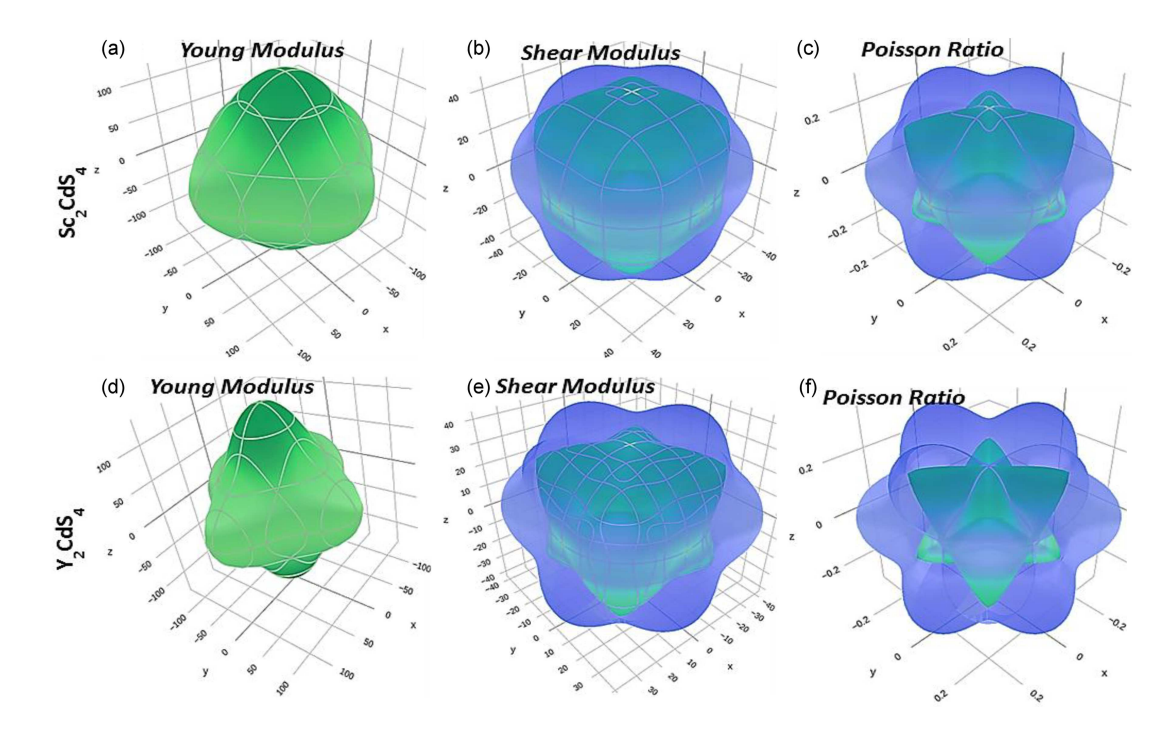


Fig. 6. (a, d) Young modulus, (b, e) shear modulus, and (c, f) Poisson ratio of the spinel Cd(Sc/Y)<sub>2</sub>S<sub>4</sub>.

For a perfect isotropic system [57], A is equal to one, hence the degree of elastic anisotropy is considered as the deviation from unity. The computed anisotropic ratio for the studied materials under investigation differs from one, as shown in Table III.

For cubic compounds, Fine et al. [58] also proposed a relationship between the melting temperature  $(T_m)$  and the elastic constant  $(C_{11})$ , namely

$$T_m = \left(500 + d_m C_{11}\right) \mp 300. \tag{10}$$

where  $d_m$  is a constant. The data in Table II shows that  $\mathrm{CdY}_2\mathrm{S}_4$  has the lowest melting temperature  $T_m$  of 1370.13 K, which is rather high for a compound that can tolerate high temperatures. The melting temperature  $T_m$  values of the other compounds are relatively high.

The Kleinman parameter  $\zeta$  [59], which quantifies the internal strain of a material, is calculated using the relation

$$\zeta = \frac{C_{11} + 8C_{12}}{7C_{11} + 2C_{12}}. (11)$$

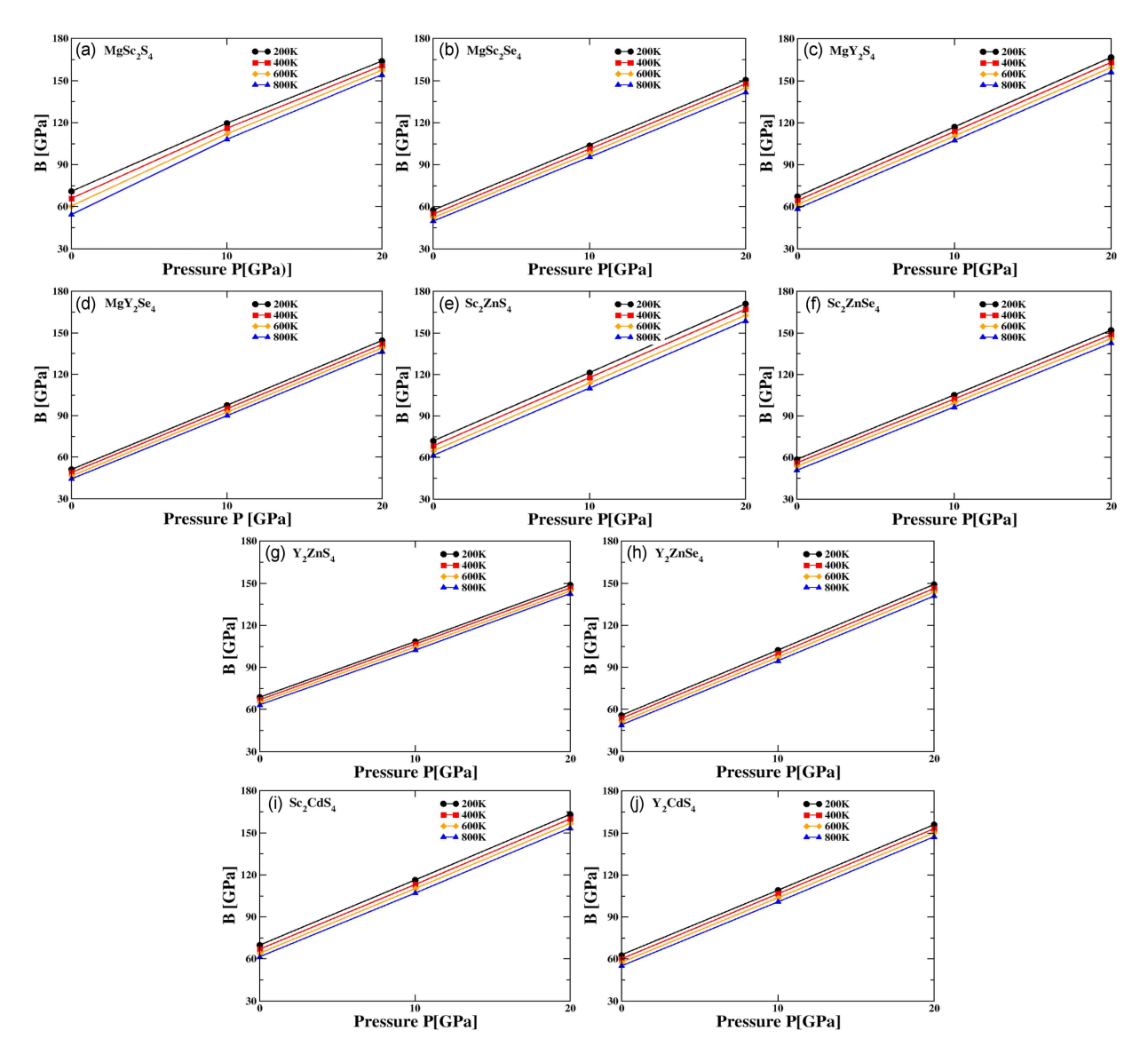


Fig. 7. Bulk modulus B [GPa] of the spinel MgA<sub>2</sub>B<sub>4</sub> (A = Sc, Y; B = S, Se), A<sub>2</sub>CdS<sub>4</sub>, and ZnA<sub>2</sub>B<sub>4</sub>.

For spinel compounds, the results given in Table III describe the relative ease of bond bending compared to bond stretching. Minimizing bond bending leads to  $\zeta=0$ , and minimizing bond stretching leads to  $\zeta=1$ . Our calculated values of the Kleinman parameter  $\zeta$  forecast that bond bending is the dominant process ( $\zeta$  falls between 0–0.5). There are no cases in our caculations where  $\zeta$  value approaches unity in the system, therefore bond stretching can be considered negligible.

For isotropic material, Lame's coefficients satisfy relations  $\lambda = C_{12}$  and  $\mu = G'$ . Since anisotropic compounds are considered in this paper, the condition for isotropic compounds is not satisfied, as can be seen from the calculated values in Table III.

The sound velocities and Debye temperature  $\Theta_{\rm D}$  [K] for the studied spinel compounds are shown in Table IV. We have determined the mean acoustic sound velocity  $(V_m)$  using the transverse

velocity  $(V_t)$  and longitudinal  $(V_l)$  velocity [60]. The obtained  $\Theta_D$  [K] values suggest that the compounds possess relatively high thermal stability over varying temperature conditions. The compound  $\text{ZnY}_2\text{Se}_4$  has  $\Theta_D = 370.56$  K, showing the compound's stability at low temperatures [61].

Table IV presents values of K (compressibility) for spinel compounds  $AB_2X_4$ . By definition, compressibility is a measure of the relative volume change in a solid in response to the mean stress or pressure changee. All materials (solids, liquids, or gases) are more or less compressible, i.e., each exhibits resistance to a change in its volume when subjected to applied stress. A material can only decrease in volume under applied pressure. The inverse of compressibility of a substance gives its bulk modulus B [GPa]. Hence, the compressibility relates to the compactness of the molecules in a material, which explains its density. Generally,

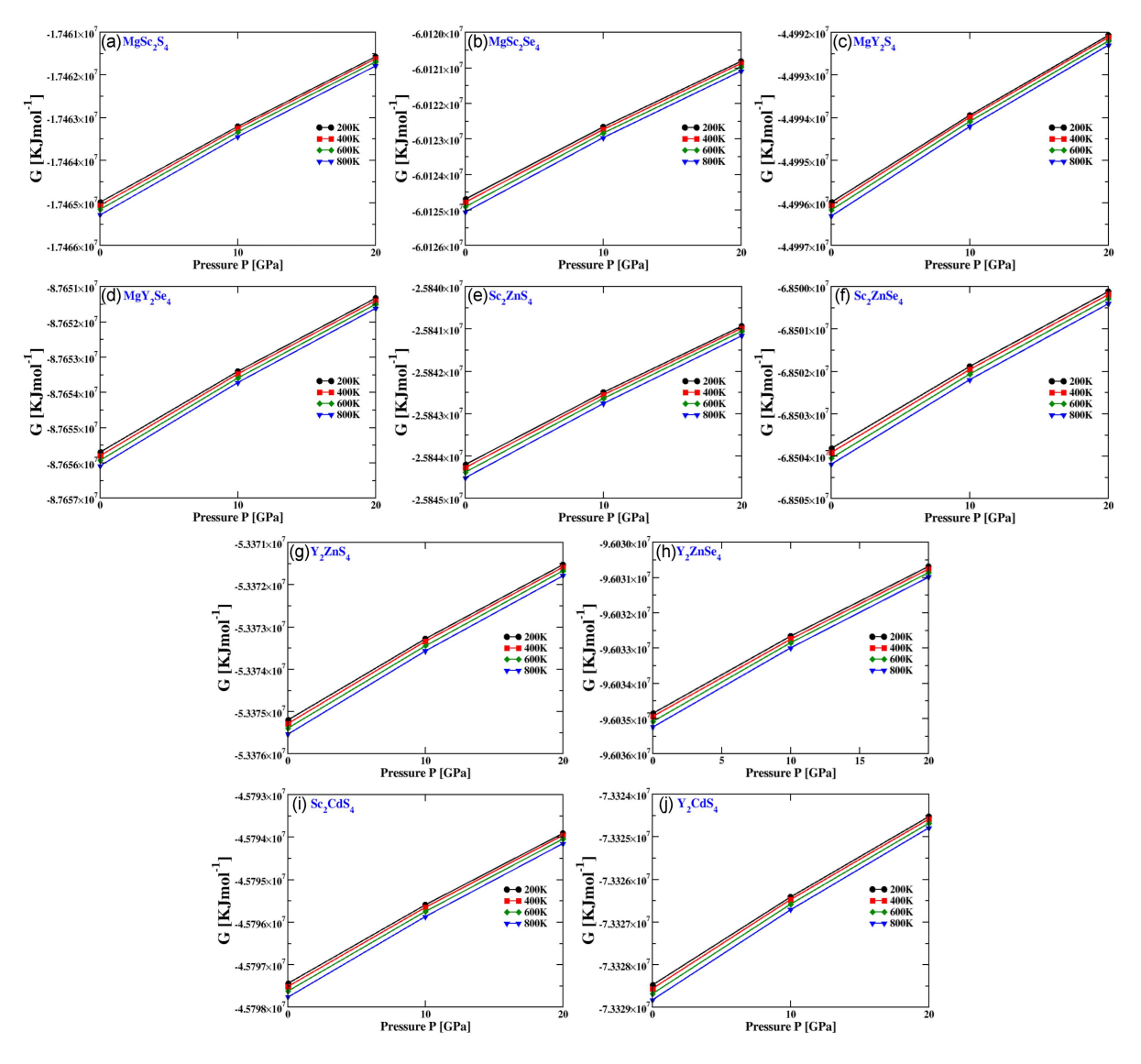


Fig. 8. Gibbs free energy G [kJ/mol] of the spinel MgA<sub>2</sub>B<sub>4</sub> (A = Sc, Y; B = S, Se), A<sub>2</sub>CdS<sub>4</sub>, and ZnA<sub>2</sub>B<sub>4</sub>.

an incompressible material has a constant density and cannot be compressed, i.e., the higher density, the lower the compressibility.

## 3.2. Thermodynamic properties

The thermodynamic (TD) properties of a material can be determined utilizing the GIBBS software [62, 63]. We relied on standard TD relationships to calculate macroscopic thermal characteristics as a function of temperature T and pressure P, with the use of the total energy E(V) for various primitive cell volumes V, measured in Sect. 3.1. The quasiharmonic Debye model, on which the GIBBS software is based, is described by the Gibbs nonequilibrium function expressed by

equinorium function expressed by
$$G^{*}\left(V:P,T\right) = E\left(V\right) + PV + A_{\mathrm{Vib}}\left(\Theta_{\mathrm{D}},T\right),\tag{12}$$

Here, the vibrational term  $A_{\text{Vib}}$  is given by

$$A_{\text{Vib}}(\Theta_{\text{D}}, T) = nk_{\text{B}}T \left[ \frac{9\Theta_{\text{D}}}{8T} + 3\ln\left(1 - e^{\frac{\Theta_{\text{D}}}{T}}\right) - D\left(\frac{\Theta_{\text{D}}}{T}\right) \right], \tag{13}$$

where n,  $k_{\rm B}$ , and D are number of atoms, Boltzmann constant, and Debye integral, respectively. In the model, the entropy is given by

$$S = nk_{\rm B}T \left[ 4D \left( \frac{\Theta_{\rm D}}{T} \right) - 3\ln \left( 1 - {\rm e}^{\frac{\Theta_{\rm D}}{T}} \right) \right]. \tag{14}$$

We studied TD characteristics in the temperature range of 200–800 K and the effects of pressure in the range of 0–20 GPa using the quasiharmonic Debye model. At the aforementioned pressure range, Figs. 7–9 illustrate how temperature affects the bulk modulus and Gibb's free energy  $G^*$  [kJ/mol] of the compounds. It is found that the bulk modulus increases sharply at a given temperature with

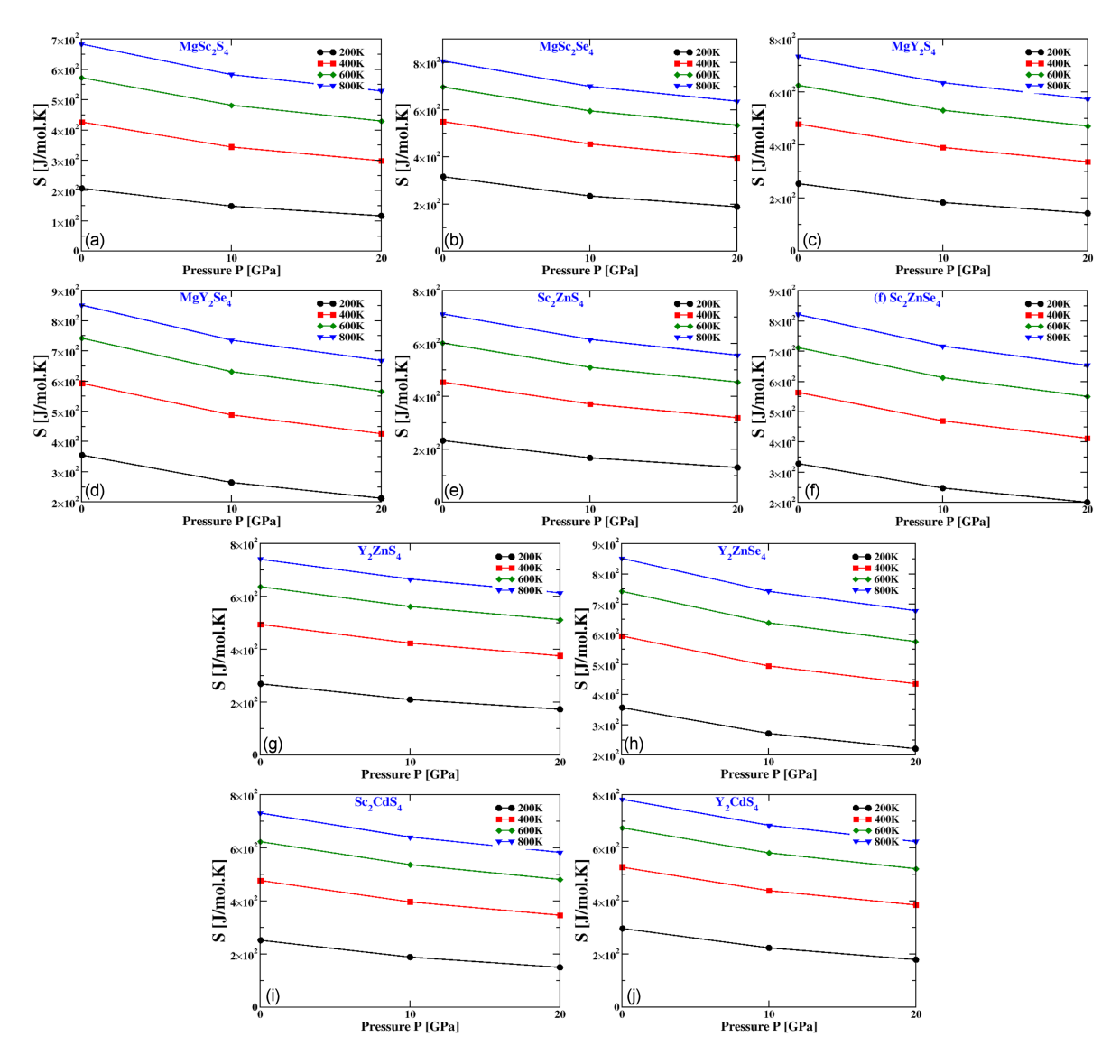


Fig. 9. Entropy S [J/(mol K)] of the spinel MgA<sub>2</sub>B<sub>4</sub> (A = Sc, Y; B = S, Se), ACd<sub>2</sub>S<sub>4</sub>, and ZnA<sub>2</sub>B<sub>4</sub>.

increasing pressure fluctuation and decreses slightly at a given pressure with increasing temperature. Figure 9a shows the change in entropy (S) as a function of pressure at various temperature ranges. It is discovered that S is weakly dependent on pressure changes and strongly dependent on temperature changes. The entropy decreases with increasing pressure and increases with increasing temperature.

### 4. Conclusions

The elastic properties of the spinels  $AB_2X_4$ , having stable cubic symmetry, were computed through a first-principles approach using the FP-LAPW technique. The lattice constants  $a_0$  [Å] are in close agreement with the experimental and other theoretical data. The elastic properties, calculated using Thomas Charpin's method and the computed

elastic constants, satisfy Born and Huang stability conditions, which confirms the mechanical stability of the compounds under study. The calculated bulk modulus for  $MgSc_2S_4$  and the Young modulus for ZnSc<sub>2</sub>S<sub>4</sub> allow us to conclude that the compounds mentioned have greater resistance to deformation. The calculated Poisson ratio and Pugh's ratio indicate the ductile nature for ZnY<sub>2</sub>Se<sub>4</sub>, while for  $MgY_2S_4$ ,  $ZnY_2S_4$ , and  $ZnY_2Se_4$  their B/G values exceed the limit > 1.75. The computed Zener anisotropic factor A, Lame constants  $\lambda$ , and  $\mu$  show anisotropic nature for the compounds under investigation, while the Kleinman parameters shows no bond stretching for them. Other mechanical properties were also investigated, such as transverse, longitudinal, and mean acoustic velocities along with the Grüensien parameter and the compound's stability calculated using the Debye temperature. The thermodynamic parameters obtained with the GIBBS2 software using the quasiharmonic model show the increase in B [GPa] and  $G^*$  [kJ/mol] and decreasing trend for S [J/(mol K)], indicating the stability of the understudied spinels compounds in the temperature range from 200 to 800 K and the pressure range from 0 to 20 GPa.

## Acknowledgments

The authors are thankful to the Deanship of Graduate Studies and Scientific Research at the University of Bisha for supporting this work through the Fast-Track Research Support Program.

#### References

- F.L. Sutherland, K. Zaw, S. Meffre, G. Giuliani, A.E. Fallick, I.T. Graham, G.B. Webb, Aust. J. Earth Sci. 56, 1003 (2009).
- [2] K. Ounnunkad, S. Phanichphant, *Mater. Res. Bull.* 47, 473 (2012).
- [3] J.F. Marco, J.R. Gancedo, M. Gracia, J.L. Gautier, E.I. Ríos, H.M. Palmer, C. Greaves, F.J. Berry, J. Mater. Chem. 11, 3087 (2001).
- [4] A. Bouhemadou, K. Haddadi, R. Khenata, D. Rached, S. Bin-Omran, *Phys. B* 407, 2295 (2012).
- [5] A.N. Naveen, P. Manimaran, S. Selladurai, J. Mater. Sci. Mater. Electron. 26, 8988 (2015).
- [6] Y. Cho, S. Lee, Y. Lee, T. Hong, J. Cho, Adv. Energy Mater. 1, 821 (2011).
- [7] A.K. Kushwaha, Ş. Uğur, S. Akbudak, G. Uğur, J. Alloys Compd. 704, 101 (2017).
- [8] Y. Liang, Y. Li, H. Wang, J. Zhou, J. Wang, T. Regier, H. Dai, *Nat. Mater.* 10, 780 (2011).
- [9] J.Y. Do, N.-K. Park, T.J. Lee, S.T. Lee, M. Kang, Int. J. Energy Res. 42, 429 (2018).
- [10] C. Wei, Z. Feng, M. Baisariyev, L. Yu, L. Zeng, T. Wu, H. Zhao, Y. Huang, M.J. Bedzyk, T. Sritharan, Z.J. Xu, *Chem. Mater.* 28, 4129 (2016).
- [11] M.S. Whittingham, *Chem. Rev.* **104**, 4271 (2004).
- [12] N. Wu, Z. Yang, H. Yao, Y. Yin, L. Gu, Y. Guo, Angew. Chem. 127, 5849 (2015).
- [13] N. Yabuuchi, K. Kubota, M. Dahbi, S. Komaba, *Chem. Rev.* **114**, 11636 (2014).
- [14] N. Zhang, F. Cheng, Y. Liu, Q. Zhao, K. Lei, C. Chen, X. Liu, J. Chen, J. Am. Chem. Soc. 138, 12894 (2016).

- [15] C. Pang, L. Gao, A.V. Singh, H. Chen, M.K. Bowman, N. Bao, L. Shen, A. Gupta, *Chem. Mater.* 30, 1701 (2018).
- [16] J. Deng, X. Yu, X. Qin, B. Liu, Y.-B. He, B. Li, F. Kang, *Energy Storage Mater.* 11, 184 (2018).
- [17] T. Irifune, K. Fujino, E. Ohtani, *Nature* **349**, 409 (1991).
- [18] S.-J. Lee, J.-E. Kim, H.Y. Park, *J. Mater. Res.* 18, 733 (2003).
- [19] H. Zhan, Y. Bian, Q. Yuan, B. Ren, A. Hursthouse, G. Zhu, *Processes* 6, 33 (2018).
- [20] C.P. Sun, C.L. Huang, C.C. Lin, J.L. Her, C.J. Ho, J.-Y. Lin, H. Berger, H.D. Yang, Appl. Phys. Lett. 96, 122109 (2010).
- [21] D. Santos-Carballal, P.E. Ngoepe, N.H. De Leeuw, *Phys. Rev. B* **97**, 085126 (2018).
- [22] P.F. Ndione, Y. Shi, V. Stevanovic, S. Lany, A. Zakutayev, P.A. Parilla, J.D. Perkins, J.J. Berry, D.S. Ginley, M.F. Toney, Adv Funct Materials 24, 610 (2014).
- [23] T. Şaşmaz Kuru, M. Kuru, S. Bağcı, J. Alloys Compd. 753, 483 (2018).
- [24] A. Govindaraj, E. Flahaut, Ch. Laurent, A. Peigney, A. Rousset, C.N.R. Rao, J. Mater. Res. 14, 2567 (1999).
- [25] Z. Lei, W. You, M. Liu, G. Zhou, T. Takata, M. Hara, K. Domen, C. Li, Chem. Commun. 2003, 2142 (2003).
- [26] N. Romeo, A. Dallaturca, R. Braglia, G. Sberveglieri, Appl. Phys. Lett. 22, 21 (1973).
- [27] A. Govindaraj, E. Flahaut, Ch. Laurent, A. Peigney, A. Rousset, C.N.R. Rao, J. Mater. Res. 14, 2567 (1999).
- [28] G. Gusmano, G. Montesperelli, E. Traversa, G. Mattogno, J. Am. Ceram. Soc. 76, 743 (1993).
- [29] N.J. van der Laag, Ph.D. Thesis, Eindhoven University of Technology, 2002.
- [30] A. Mahmood, W. Guo, H. Tabassum, R. Zou, Adv. Energy Mater. 6, 1600423 (2016).
- [31] R.J. Hill, J.R. Craig, G.V. Gibbs, *Phys. Chem. Miner.* 4, 317 (1979).
- [32] S. Jiang, T. Lu, Y. Long, J. Chen, J. Appl. Phys. 111, 043516 (2012).
- [33] S.I. Radautsan, I.M. Tiginyanu, *Jpn. J. Appl. Phys.* **32**, 5 (1993).
- [34] D. Santamaría-Pérez, M. Amboage, F.J. Manjón, D. Errandonea, A. Muñoz, P. Rodríguez-Hernández, A. Mújica, S. Radescu, V.V. Ursaki, I.M. Tiginyanu, J. Phys. Chem. C 116, 14078 (2012).

- [35] G.M. Mustafa, N.A. Noor, M.W. Iqbal, M. Sajjad, M.A. Naeem, Q. Mahmood, H.M. Shaikh, A. Mahmood, W. Al-Masry, Mat. Sci. Semicon. Proc. 121, 105452 (2021).
- [36] L. Ali, R. Neffati, A. Muhammad, M. Ullah, M.W. Ashraf, M. Haneef, G. Murtaza, Phys. Scr. 98, 015802 (2023).
- [37] L. Wang, Z. Zhao-Karger, F. Klein, J. Chable, T. Braun, A.R. Schür, C. Wang, Y. Guo, M. Fichtner, *ChemSus Chem* 12, 2286 (2019).
- [38] P. Canepa, G. Sai Gautam, D. Broberg, S.-H. Bo, G. Ceder, *Chem. Mater.* 29, 9657 (2017).
- [39] R. Ali, G.-J. Hou, Z.-G. Zhu, Q.-B. Yan, Q.-R. Zheng, G. Su, J. Mater. Chem. A 6, 9220 (2018).
- [40] P. Blaha, K. Schwarz, P. Sorantin, S.B. Trickey, Comput. Phys. Commun. 59, 399 (1990).
- [41] P. Blaha, K. Schwarz, G.K.H. Madsen, D. Kvasnicka, J. Luitz, R. Laskowski, F. Tran, L.D. Marks, WIEN2k: An Augmented Plane Wave Plus Local Orbitals Program for Calculating Crystal Properties, Karlheinz Schwarz, Techn. Universität Wien, Austria 2018.
- [42] J.P. Perdew, K. Burke, M. Ernzerhof, *Phys. Rev. Lett.* 77, 3865 (1996).
- [43] M.G. Brik, A. Suchocki, A. Kamińska, Inorg. Chem. 53, 5088 (2014).
- [44] J. Flahaut, M. Guittard, M. Patrie, M.P. Pardo, S.M. Golabi, L. Domange, Acta Cryst. 19, 14 (1965).
- [45] L.-P. Wang, Z. Zhao-Karger, F. Klein, J. Chable, T. Braun, A.R. Schür, C. Wang, Y. Guo, M. Fichtner, *ChemSusChem* 12, 2286 (2019).
- [46] P. Canepa, G. Sai Gautam, D. Broberg,
   S.-H. Bo, G. Ceder, *Chem. Mater.* 29, 9657 (2017).
- [47] P. Canepa, S.-H. Bo, G. Sai Gautam, B. Key, W.D. Richards, T. Shi, Y. Tian, Y. Wang, J. Li, G. Ceder, *Nat. Commun.* 8, 1759 (2017).

- [48] A.K. Kushwaha, A. Bouhemadou, R. Khenata, A. Candan, S. Akbudak, Ş. Uğur, Comput. Condens. Matter 21, e00428 (2019).
- [49] A. Mahmood, S.M. Ramay, W. Al-Masry, A.A. Al-Zahrani, N.Y.A. Al-Garadi, *Mod. Phys. Lett. B* 35, 2150184 (2021).
- [50] T. Alshahrani, G.M. Mustafa, T.H. Flemban, H. Althib, S. Al-Qaisi, N.A. Kattan, Q. Mahmood, ECS J. Solid State Sci. Technol. 9, 105001 (2020).
- [51] F. Tasnádi, M. Odén, I.A. Abrikosov, *Phys. Rev. B* 85, 144112 (2012).
- [52] K. Tibane, P. Ngoepe, C. Masedi, MATEC Web Conf. 388, 07014 (2023).
- [53] K. Bouferrache M.A. Ghebouli, Y. Slimani, B. Ghebouli, M. Fatmi, T. Chihi, M.A. Habila, N.H. Alotaibi, M. Sillanpaa, Bull. Mater. Sci. 47, 102 (2024).
- [54] E. Biagi, E. Borchi, S.D. Gennaro, L. Masi, J. Phys. D Appl. Phys. 25, 901 (1992).
- [55] V. V. Bannikov, I.R. Shein, A.L. Ivanovskii, Phys. Status Solidi Rapid Res. Lett. 1, 89 (2007).
- [56] F. Tasnádi, M. Odén, I.A. Abrikosov, *Phys. Rev. B* 85, 144112 (2012).
- [57] C. Nianyi, L. Chonghe, Y. Shuwen, W. Xueye, J. Alloys Compd. 234, 130 (1996).
- [58] M.E. Fine, L.D. Brown, H.L. Marcus, Scr Metall. 18, 951 (1984).
- [59] S.F. Pugh, Lond. Edinb. Dubl. Philos. Mag. J. Sci. 45, 823 (1954).
- [60] S. Al-Qaisi, R. Ahmed, B. Ul Haq, D.P. Rai, S.A. Tahir, *Mater. Chem. Phys.* 250, 123148 (2020).
- [61] P. Wachter, M. Filzmoser, J. Rebizant, Physica B 293, 199 (2001).
- [62] M.A. Blanco, E. Francisco, V. Luaña, Comput. Phys. Commun. 158, 57 (2004).
- [63] K. Deepthi Jayan, V. Sebastian, *Mater. Today Commun.* **28**, 102650 (2021).